Acta Chemica Scandinavica, 1995: 49: 411–416
Printed in Belgium – all rights reserved

ACTA
CHEMICA SCANDINAVICA
ISSN 0904–213X

Surface Tension of Binary MF–AlF_3 (M = Li, Rb, Cs) Melts

Vladimir Danek[a] and Terje Østvold[†,b]

[a] Institute of Inorganic Chemistry, Slovak Academy of Sciences, Dubravska cesta 9, 842 36 Bratislava, Slovakia and [b] Institute of Inorganic Chemistry, The Norwegian Institute of Technology, N-7034 Trondheim, Norway

Danek, V. and Østvold, T., 1995. Surface Tension of Binary MF–AlF_3 (M = Li, Rb, Cs) Melts. – Acta Chem. Scand. 49: 411–416 © Acta Chemica Scandinavica 1995.

The surface tension of the molten systems MF–AlF_3, where M = Li, Rb, Cs, has been determined using the maximum bubble pressure method. The total error in the surface tension measurement was estimated to be ± 1%.

In all the investigated systems the surface tension decreases with increasing concentration of AlF_3. This is apparently due to the formation of components such as $MAlF_4$ having stronger covalent character than the pure ionic MF melt. Owing to their covalent character these components will concentrate on the surface of the melt.

The relative surface entropy has a maximum which is shifted towards higher AlF_3 concentrations when increasing the size of the alkali metal ion. This reflects the relatively simple structure of the pure MF and $MAlF_4$ melts consisting mainly of M^+, F^- and M^+ and AlF_4^- relative to melts in the range $0 < x_{AlF_3} < 0.5$, where the concentration of the ions AlF_6^{3-}, AlF_5^{2-} and AlF_4^- are changing considerably. The above-mentioned maximum is reduced in the sequence Li > Na > (K, Rb, Cs), indicating higher ordering for the KF, RbF and CsF than for the NaF- and LiF-containing MF–AlF_3 melts.

In spite of extensive investigations over six decades the structure of melts based on cryolite, Na_3AlF_6, is still not sufficiently understood. The most accepted dissociation scheme of molten cryolite is the one given below:[1]

$$Na_3AlF_6 = 3\,Na^+ + AlF_6^{3-} \quad (1)$$

$$AlF_6^{3-} = AlF_4^- + 2\,F^- \quad (2)$$

This dissociation scheme was recently modified by Dewing.[2] This was done no explain some discrepancies in the heat capacity of the NaF–AlF_3 mixtures and the dissociation constant calculated on the basis of thermodynamic[1] and spectroscopic[3] data. Dewing proposed the following reactions:

$$AlF_6^{3-} = AlF_5^{2-} + F^- \quad (3)$$

$$AlF_5^{2-} = AlF_4^- + F^- \quad (4)$$

He also found that AlF_5^{2-} is the most abundant anionic species at the $x_{AlF_3} = 0.33$ composition. The existence of the AlF_5^{2-} anion in the liquid state was also postulated by Xiang and Kvande[4] on the basis of liquidus temperature calculations and Gilbert and Materne[5] using Raman spectroscopy. An attempt to confirm the presence of the AlF_5^{2-} anion in the MF–AlF_3 (M = Li, Na, K) melts on the basis of vapour-pressure measurements was also made by Zhou.[6]

Surface-tension data of a melt reflect the nature of chemical bonding between species occurring in the liquid. There will be a difference in bonding between the different species present in MF–AlF_3 melts owing to their difference in charge and size. Species having more covalent character will become surface active and will concentrate on the surface of the melt. Therefore the composition of species, especially the content of acid components such as $NaAlF_4$, having the strongest covalent character for melts with $x_{AlF_3} \leq 0.5$, will influence substantially the concentration dependence of the surface tension of these binary melts. The dissociation mechanism of M_3AlF_6 may be substantially influenced by the size and polarization ability of different M^+ cations. Since the polarization ability of the alkali metal cations decreases from lithium to caesium, it may be supposed that the degree of dissociation of the AlF_6^{3-} anion will decrease in the same manner. Dewing[2] has reported that the AlF_5^{2-} ion may not form in LiF–AlF_3 melts, while AlF_5^{2-} may be a major anion in NaF–AlF_3 melts, However, recent Raman Spectroscopic data[7] indicate that there are insignificant differences in the anionic distributions in MF–AlF_3 (M = Li, Na, K) melts for $x_{AlF_3} < 0.5$.

In the present work the surface tension of the MF–AlF_3 (M = Li, Rb, Cs) melts has been measured using the maximum bubble pressure method. The surface tension of these systems has not been studied till now. The concentration dependencies of the surface tension of the investigated systems are compared with those of the so-

† To whom correspondence should be addressed.

dium and potassium systems measured previously[8] and discussed in terms of the anionic composition.

Experimental

Apparatus. The apparatus consisted of a resistance furnace provided with an adjustable head fixing the position of the platinum capillary, the Pt/PtRh10 thermocouple and a platinum wire which served as an electric contact to adjust the exact touch of the capillary with the liquid surface.

The Microcor temperature controller adjusted the needed operational constants for the temperature control of the furnace using an additional Pt/PtRh10 control thermocouple placed in between the working and heating shafts of the furnace. The digital programmer Palcor RNZ enabled us to use any temperature program. A Solatron voltmeter was used for temperature measurements.

The platinum capillary with an outer diameter of 3 mm had two different inner diameters one at each end. In order to obtain precise results, the capillary tip was carefully machined. The orifice had to be as circular as possible, with a sharp conical edge. A precise inner diameter of the capillary is very important if accurate measurements are to be performed. A Reichert MeF3A microscope was used to measure the diameter of the orifice. On one end the orifice diameter was 1.139 mm, on the other end 2.014 mm. The higher diameter was used in those melts where the bubble exerted a high adhesion to platinum. This effect was observed in $LiF-AlF_3$ melts with high AlF_3 contents. The actual capillary radius at a given temperature was calculated using the thermal expansion data for platinum.

A special water-cooled furnace lid was used for the capillary support. A micrometer screw, fixed on the lid, determined the position for the exact touch of the capillary with the liquid surface and gave the desired immersion depth with an accuracy of 0.01 mm.

A digital micromanometer (Commet LB/ST 1000) with two measuring ranges, 200 and 1000 Pa, was used for pressure measurements. This enabled us to measure the pressure with an accuracy of $\pm$ 1 Pa. Nitrogen was used to form the bubbles and to maintain an inert atmosphere over the sample. The gas was slowly fed through the capillary during the experiment to avoid condensation in the upper part of the capillary. The nitrogen flow was adjusted using a fine needle valve. The rate of bubble formation was ca. 1 bubble in 20–30 s.

Procedure. The surface tension may be calculated according to the equation[9]

$$\sigma = \frac{r}{2}(p_{max} - ghd) \qquad (5)$$

where r is the capillary radius, p_{max} is the maximum bubble pressure when the bubble is a hemisphere of radius equal to the capillary radius, g is the gravitational constant, h is the depth of immersion of the capillary and d is the density of the melt. However, there is also a possibility of calculating the surface tension of the liquid without knowing the density of the melt. By eliminating the density, d, from eqn. (5) for two different immersion depths we obtain the equation

$$\sigma = \frac{r}{2}\,\frac{p_{max,1}h_2 - p_{max,2}h_1}{h_2 - h_1} \qquad (6)$$

where $p_{max,i}$, is the maximum bubble pressure at immersion depth h_i. Since the density data for the rubidium and caesium systems are not known, we used eqn. (6) for these melts.

The surface tension of each sample was measured at 5–7 different temperatures in a range of 100–120 °C starting ca. 20 °C above the temperature of primary crystallisation, T_m, which was obtained from the literature.[10] The measurements were carried out at four different depths of immersion (usually 2, 3, 4 and 5 mm) yeilding six surface tension values for each temperature.

The temperature dependence of the surface tension can be expressed by the linear equation

$$\sigma = a - bT \qquad (7)$$

where σ is the surface tension in mN m^{-1} and T is the temperature in °C.

Precision and accuracy. In surface tension measurements using the maximum bubble pressure method several sources of error may occur. As mentioned above, the exact machining of the capillary orifice is important. A deviation from a circular orifice in our case caused an error of $\pm$0.3%. The determination of the immersion depth with an accuracy of $\pm$0.01 mm introduced an error of $\pm$0.3%. The accuracy of $\pm$ 1 Pa in the pressure measurement caused an additional error of $\pm$0.4%. The sum of all these errors gives an estimated total error of ca. $\pm$1%. The standard deviations of the experimental data

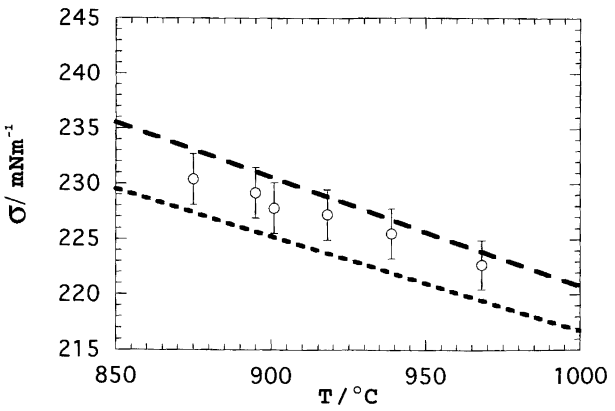

Fig. 1. Temperature dependence of the surface tension of LiF: (○) this work, SD = 1%; (– – –) Ref. 11; (·····) Ref. 8.

Table 1. Depth of immersion, measured maximum bubble pressure and calculated surface tension of liquid LiF at different temperatures.

t/°C	h/mm	p_{max}/p_a	σ/mN m^{-1}		
968	2	814			
	3	832	222.4		
	4	850	222.4	222.4	
	5	867	222.6	222.8	223.5
939	2	825			
	3	843	225.5		
	4	861	225.5	225.5	
	5	879	225.5	225.5	225.5
918	2	830			
	3	848	226.9		
	4	866	226.9	226.9	
	5	883	227.1	227.3	228.1
901	2	836			
	3	854	228.6		
	4	873	228.3	227.8	
	5	893	228.0	227.3	229.6
895	2	838			
	3	856	229.2		
	4	874	229.2	229.2	
	5	892	229.2	229.2	229.2
875	2	843			
	3	862	230.9		
	4	881	230.6	230.0	
	5	900	230.5	230.0	230.0

based on the least-squares statistical analysis were in the range ±0.5–1%.

The experimental set-up was checked by measuring the surface tension of pure molten salts with known surface tension. Molten NaCl, LiF, NaF, KF, RbF and CsF were selected. A typical data set for LiF is given in Table 1 and in Fig. 1. The coefficients a and b in eqn. (7) and the standard deviation of the fit for the selected pure melts are given in Table 2. A comparison of the obtained data with those given by Janz *et al.*[11] is given in Table 3. Very good agreement with literature data within the estimated experimental error of ±1% is confirmed. The only exception is caesium and rubidium fluoride, where the reference data may have to be revised.

Chemicals. Chemicals and purification procedures are given below: NaCl, LiF, NaF, KF: all p.a., Merck AG, dried at 600°C for 6 h; RbF: Johnson and Matthey, Karlsruhe selected crystals recrystallized twice in a Pt crucible under nitrogen; CsF: 99.9% Ventron, GmbH, Karlsruhe, dried at 600°C; CsF: p.a., Fluka recrystallized twice in Pt crucible under nitrogen; AlF_3: technical grade, sublimated in vacuum in a graphite crucible.

All handling and storage of salts were done in a glove box with a moisture content lower than 10 ppm.

Table 3. A comparison between the present surface tension data and literature values for some selected pure melts.

Compound	T/°C	σ/mN m^{-1} Ref. 11	σ/mN m^{-1} This work	Difference (%)
NaCl	850	110.4	110.4	0.0
LiF	900	230.6	228.5	−0.9
NaF	1000	185.2	185.8	0.3
KF	900	140.6	140.4	−0.1
RbF	850	121.2	118.9	−1.9
CsF[a]	800	97.9	97.4	−0.5
CsF[b]	800	97.9	100.7	+2.9

[a] Dried. [b] Recrystallized.

Results and disussion

The coefficients a and b in eqn. (7) as well as the standard deviations of the fit for the investigated MF–AlF_3 systems are given in Table 4. Some isotherms of the surface tension of the systems LiF–AlF_3, RbF–AlF_3 and CsF–AlF_3 are presented in Figs. 2, 3 and 4, respectively.

For all the systems investigated the surface tension decreased with increasing concentration of AlF_3. This behaviour may be explained by the formation of more covalent compounds in the melt with increasing concentration of AlF_3. Owing to their covalent character these compounds will concentrate on the surface of the melt. There is, however, a marked change in the concentration dependence of the surface tension on going from LiF to CsF. This change may be observed when comparing the present data shown in Figs. 2–4 with previously published results shown in Fig. 5 for the NaF–AlF_3 and KF–AlF_3 binaries.[8] While the data for the Li, Na and K systems show a continuous change in surface tension versus composition, there is a tendency in the surface tension data for the RbF–AlF_3 and CsF–AlF_3 binaries to indicate compound formation at the $x_{AlF_3} = 0.25$

Table 2. Coefficients a and b in eqn. (7) and the standard deviation of the fit, SD, for some selected pure salts.

Compound	a/mN m^{-1}	b/mN m^{-1} °C^{-1}	SD/mN m^{-1}	Temp. range/°C
NaCl	176.8	0.0781	0.6	848–917
LiF	301.6	0.0814	0.5	875–968
NaF	288.1	0.1023	0.5	1001–1086
KF	214.6	0.0824	1.7	863–942
RbF	186.6	0.0796	0.6	787–915
CsF[a]	157.2	0.0747	0.5	731–859
CsF[b]	160.6	0.0748	0.9	734–817

[a] Dried. [b] Recrystallized.

Table 4. Coefficients *a* and *b* in eqn. (7) and the standard deviations of the fit for MF-AlF_3 (M=Li, Rb, Cs) melts.

x_{AlF_3}	a/mN m^{-1}	b/mN m^{-1} °C^{-1}	SD/mN m^{-1}	Temp. range/°C
LiF–AlF_3				
0.00	301.6	0.0814	0.6	875–968
0.05	359.1	0.1558	0.7	848–935
0.10	403.0	0.2173	1.0	838–940
0.15	398.9	0.2290	1.1	765–895
0.20	339.6	0.1907	1.0	788–899
0.25	284.7	0.1543	0.7	808–917
0.30	273.4	0.1595	0.8	790–907
0.40	167.7	0.0741	1.1	815–934
0.50	86.2	–	1.5	995
RbF–AlF_3				
0.000	186.6	0.0796	0.6	787–915
0.099	191.5	0.0921	0.4	846–945
0.193	197.5	0.1065	0.6	941–1038
0.210	200.9	0.1109	0.6	956–1035
0.239	202.5	0.1141	0.7	986–1086
0.242	201.3	0.1116	0.7	994–1098
0.256	191.6	0.1039	0.8	988–1116
0.291	170.3	0.0986	0.5	928–1033
0.318	146.6	0.0839	1.0	1015–1077
0.395	125.5	0.0768	0.4	835–940
0.500	90.4	0.0487	1.2	829–935
CsF–AlF_3				
0.000	157.2	0.0747	0.5	731–859
0.000	160.6	0.0748	0.9	734–817
0.096	173.1	0.1028	0.7	745–845
0.193	171.2	0.1064	0.3	827–935
0.210	174.2	0.1090	0.9	844–947
0.229	167.7	0.1056	0.5	835–937
0.230	171.1	0.1056	0.6	843–947
0.235	166.6	0.1026	0.6	835–943
0.250	167.0	0.1016	0.6	845–948
0.270	164.2	0.1016	0.6	824–927
0.278	164.2	0.1068	0.5	808–904
0.290	159.6	0.1026	1.2	787–889
0.398	116.9	0.0778	0.7	735–851
0.471	87.6	0.0512	0.6	833–944
0.500	82.9	0.0460	0.5	787–898

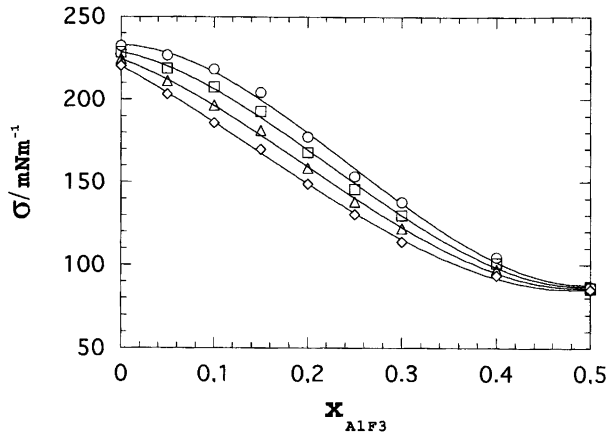

Fig. 2. Surface tension isotherms of the system LiF–AlF_3: (○) 850, (□) 900, (△) 950, (◇) 1000°C.

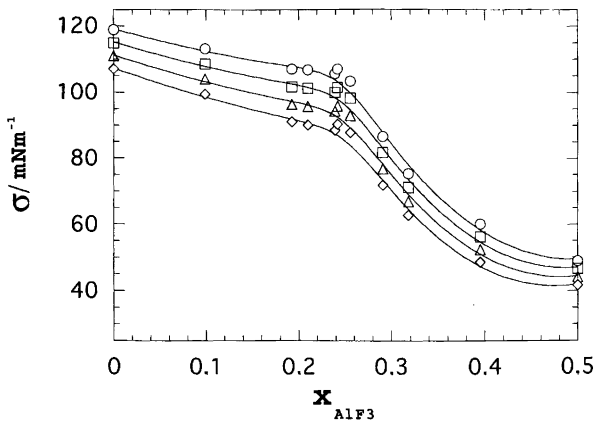

Fig. 3. Surface tension isotherms of the system RbF–AlF_3: (○) 850, (□) 900, (△) 950, (◇) 1000°C.

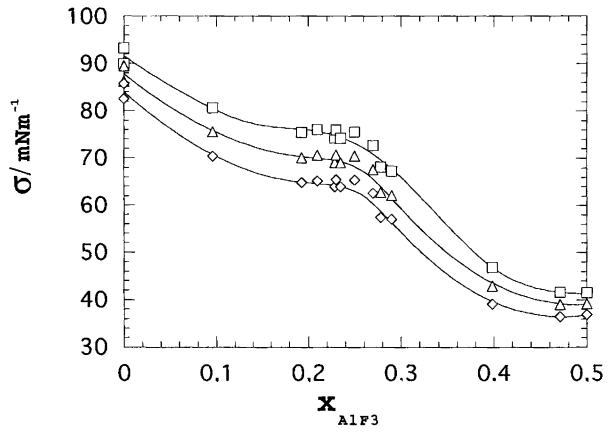

Fig. 4. Surface tension isotherms of the system $CsF–AlF_3$: (□) 900, (△) 950, (◇) 1000°C.

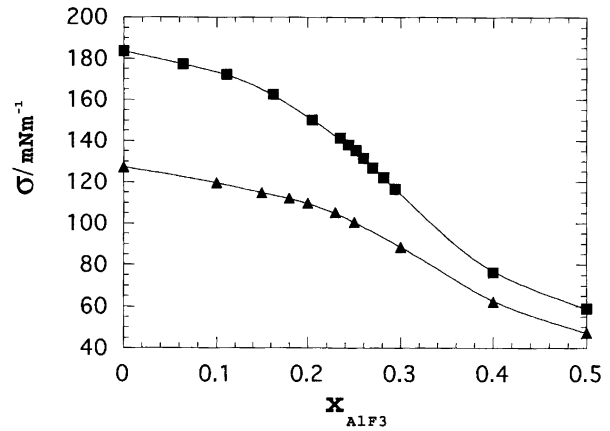

Fig. 5. Surface tension versus x_{AlF_3} at 1000°C: (■) $NaF–AlF_3$, (▲) $KF–AlF_3$.[8]

composition. This may be interpreted as an increasing tendency to stabilize the M_3AlF_6 compound when increasing the size of the alkali metal ion. This tendency is, however, not observed in Raman studies of $MF–AlF_3$ (M = Li, Na and K) melts,[7] where the AlF_6^{3-} ion seems to dissociate to the same degree in all three binaries. The above hypothesis is also in disagreement with the thermodynamic study of Hehua Zhou,[6] who observed a strong dissociation tendency of the AlF_6^{3-} ion for both Na_3AlF_6 and K_3AlF_6 melts. On the other hand, the phase diagrams of the $RbF–AlF_3$ and $CsF–AlF_3$ systems show sharp maxima at the Rb_3AlF_6 and Cs_3AlF_6 compositions, respectively,[12] indicating high stability of the AlF_6^{3-} ion.

For a system in equilibrium Gibbs' equation for the surface tension is valid:[13]

$$d\sigma = -S^s dT - \Sigma\Gamma_i d\mu_i \qquad (8)$$

In this equation S^s is the surface entropy, Γ_i is the relative surface adsorption and μ_i is the chemical potential of component i. The Gibbs equation enables us to calculate the surface entropy, S^s from the temperature dependence of the surface tension:

$$S^s = -\left(\frac{d\sigma}{dT}\right)_{\mu_j} \qquad (9)$$

The surface entropy is related to the structure and the distribution of species on the surface. Hence this property will also be related to the distribution of ions in the bulk owing to equilibrium between surface and bulk. There is, however, no simple relation between the composition of the surface and the bulk owing to the preference for species with covalent character to concentrate on the surface.

Comparing eqns. (7) and (9) we see that the surface entropy is equal to the coefficient b in eqn. (7). In Fig. 6 a plot of the surface entropy versus x_{AlF_3} is shown. The surface entropy seems to have a maximum that is shifted to higher AlF_3 concentrations when increasing the size of the alkali metal. This maximum reflects the relatively simple structure of the pure MF and $MAlF_4$ melts in comparison with melts having $0 < x_{AlF_3} < 0.5$. Simultaneously this maximum decreases and becomes broader in the sequence Li→Cs. This behaviour is probably due to a more ordered structure for the KF, RbF and CsF than for the NaF and LiF containing $MF–AlF_3$ melts. Both the Li^+ and Na^+ ion will have a much stronger polarizing power than the larger alkali metal ions. This may lead to a higher degree of distortion of the complex anions formed in the Li^+- and Na^+-containing melts than for melts containing K^+, Rb^+ and Cs^+. Such effects are observed for $AlCl_4^-$ and $Al_2Cl_7^-$ in chloride melts.[14] Such disorder may be reflected in a higher melt entropy and could be one reason for the higher surface entropy observed for melts with the smaller alkali metal cation.

In conclusion we may remark that the data we have presented give some insights into the structure of $MF–AlF_3$ (M = Li, Na, K, Rb, Cs) melts. However, Raman data have shown that the structure of these melts is very

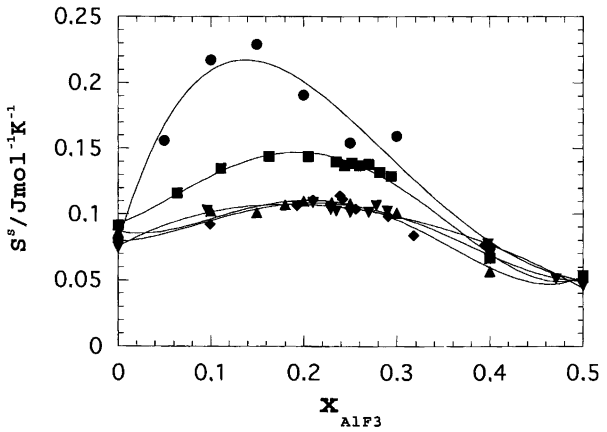

Fig. 6. Surface entropy versus x_{AlF_3} for the systems $MF–AlF_3$: (●) $LiF–AlF_3$, (■) $NaF–AlF_3$,[8] (▲) $KF–AlF_3$,[8] (◆) $RbF–AlF_3$, (▼) $CsF–AlF_3$.

complex, and more work is needed to reach an understanding of how the complex structure of these melts varies with the size of the alkali metal ions and composition, and how this melt structure influences surface properties.

Acknowledgement. V.D. stayed at the Institute of Inorganic Chemistry, NTH, in Trondheim for three months in 1992. This stay was supported by The Strong Point Center of Light Metals Production at The Institute of Inorganic Chemistry, NTH, Trondheim. Some of the present experimental data were obtained by Beatrice Schroetter, a visiting student from the University of Aachen.

References

1. Grjotheim, K., Krohn, C., Malinovsky, M., Matiasovsky, K. and Thonstad, J. *Aluminium Electrolysis: The Chemistry of the Hall–Heroult Process*, 2nd edn., Aluminium-Verlag GmbH, Düsseldorf 1982, p. 91.
2. Dewing, E. W. *Proc. Electrochem. Soc. 86* (1986) 262.
3. Gilbert, B., Mamantov, G. and Begun, G. M. *J. Chem. Phys. 62* (1975) 950.
4. Xiang, T. N. and Kvande, H. *Acta Chem. Scand., Ser. A40* (1986) 622.
5. Gilbert, B. and Materne, T. *Appl. Spectroscopy 44* (1990) 299.
6. Zhou, Hehua. *Dr.ing. Thesis No. 63*, Institute of Inorganic Chemistry, Norwegian Institute of Technology, Trondheim 1991.
7. Gilbert, B. *Personal communication.*
8. Fernandez, R. and Østvold, T. *Acta Chem. Scand. 43* (1989) 151.
9. Adamson, A. W. *Physical Chemistry of Surfaces*, New York 1960.
10. Janz, G. J. and Tomkins, R. P. T. *Phys. Prop. Data Comp. Relevant to Energy Storage IV. Molten Salts: Data on Additional Single and Multicomparent Salt Systems*, NSRDS-NBS 61, Part VI, Washington 1981.
11. Janz, G. J. *J. Phys. Chem. Ref. Data 17, Suppl. 2* (1988).
12. Puschin, N. and Baskow, A. Z. *Anorg. Chem. 81* (1913) 356.
13. Defay, R., Prigogine, I., Bellemans, A. and Everett, D. H. *Surface Tension and Adsorption*, Longmans, London 1966.
14. Einarsrud, M.-A. *Dr.ing. Thesis No. 52*, Institute of Inorganic Chemistry, Norwegian Institute of Technology, Trondheim 1987.

Received November 4, 1994.